




Isotherm and kinetic studies for heptachlor removal from aqueous solution using Fe/Cu nanoparticles, artificial intelligence, and regression analysis

Ahmed S. Mahmoud, Aya Ismail, Mohamed K. Mostafa, M. S. Mahmoud, Wageh Ali & Amira M. Shawky

To cite this article: Ahmed S. Mahmoud, Aya Ismail, Mohamed K. Mostafa, M. S. Mahmoud, Wageh Ali & Amira M. Shawky (2019): Isotherm and kinetic studies for heptachlor removal from aqueous solution using Fe/Cu nanoparticles, artificial intelligence, and regression analysis, Separation Science and Technology

To link to this article: <https://doi.org/10.1080/01496395.2019.1574832>

 View supplementary material 



 Published online: 12 Feb 2019.

 Submit your article to this journal 

 View Crossmark data 



Isotherm and kinetic studies for heptachlor removal from aqueous solution using Fe/Cu nanoparticles, artificial intelligence, and regression analysis

Ahmed S. Mahmoud ^a, Aya Ismail^a, Mohamed K. Mostafa ^{b,c}, M. S. Mahmoud^a, Wageh Ali^a, and Amira M. Shawky^a

^aSanitary and Environmental Institute (SEI), Housing and Building National Research Center (HBRC), Cairo, Egypt; ^bFaculty of Engineering and Technology, Badr University in Cairo, Cairo, Egypt; ^cEnvironmental Engineering Program, Zewail City of Science and Technology, Cairo, Egypt

ABSTRACT

This study was conducted to investigate the removal efficiency of heptachlor from aqueous solutions using bimetallic iron/copper (Fe/Cu) nanoparticles. The highest removal efficiency of 99.3% for heptachlor compounds was achieved at pH 7.0, bimetallic Fe/Cu dosage 0.33 g/L, initial heptachlor concentration 2 µg/L, contact time 30 min, and stirring rate 250 rpm. The adsorption data of heptachlor fitted well to Koble–Corrigan isotherm and Avrami kinetic model. Artificial neural network r^2 : 0.9567) was more precise than the response surface methodology (r^2 : 0.774) in simulating the adsorption of heptachlor onto the bimetallic Fe/Cu nanoparticles. This study indicated that bimetallic Fe/Cu could be employed as an efficient adsorbent for the removal of heptachlor compound.

ARTICLE HISTORY

Received 27 September 2018
Accepted 23 January 2019

KEYWORDS

Adsorption and degradation; artificial neural network and response surface methodology; chlorinated pesticides; bimetallic Fe/Cu nanoparticles; heptachlor; isotherms and kinetics

Introduction

Chlorinated pesticides are semi-volatile organic compounds and part of persistent organic pollutants (POPs).^[1] They are commonly used as pesticides due to their simplicity, rapidity, low cost, and high efficiency.^[2] POPs contain nine compounds from organochlorine pesticides.^[3] Organochlorines have been of great concern due to their occurrence in high concentrations even in remote ecosystems, despite bans on production and usage. Organochlorine compounds have a negative effect on reproduction cycle of human and animals and can cause hormonal problems.^[4] Heptachlor is one of the organochlorine compounds, which is characterized by high toxicity.^[5] It exists in surface water, wastewater, contaminated soil, and groundwater.^[6] Because of its toxicity, the World Health Organization has separated heptachlor and heptachlor epoxide from organochlorine pesticide that are listed in the allowable drinking water limits (not exceeding 0.03 µg/L) although the allowed limits for other organochlorine pesticides compounds range from 1 to 20 µg/L.^[7] Recent years have witnessed an excessive use of pesticides, especially in developing countries, which led to an increase in heptachlor concentration in surface water. For example, one of the agricultural drains in Egypt called “Mahsama,” was suffering from high concentration of heptachlor, which has a direct effect on aquatic life and human health. Moraes

et al.^[8] have collected water, sediment, and fish samples from different rivers in Brazil, and they have reported that the concentration of heptachlor in five sites were above the regulatory concentration for protection of aquatic life. Additionally, heptachlor compounds were present in all analyzed sediment samples, as well as in all fish samples. The results of another study showed that heptachlor could cause DNA damage, which may lead to mammary cancer.^[9]

The removal of organochlorine pesticides especially heptachlor compound was studied using different techniques, such as degradation and adsorption methods.^[10,11] These techniques include electro coagulation, enzymes, bacteria, and nanotechnology.^[12–14] Nanocatalysts technology, such as zero-valence metal, semiconductor materials, and bimetallic nanoparticles, has been widely used in wastewater treatment due to their reactivity and high surface area.^[15] Bimetallic iron/copper (Fe/Cu) has proved to be effective in the removal of many organic compounds, such as chlorinated ethane, chlorinated hydrocarbons, poly and mono aromatic hydrocarbons, and polychlorinated biphenyls.^[15,16] The removal of heptachlor compound using bimetallic nanoparticles undergoes two main processes: reductive degradation process and adsorption process. For this reason, bimetallic is preferred for dechlorination or reduction followed by

adsorption of organic compounds.^[17] Cao *et al.*^[18] have reported a high reductive efficiency about 90% for dechlorination of 1, 2, 4-trichlorobenzene using mono dispersed carboxy methyl cellulose-stabilized Fe–Cu bimetal nanoparticles. Therefore, the adsorption of heptachlor from aqueous solutions onto bimetallic Fe/Cu can be a viable research topic.

Many environmental factors, such as adsorbent dosage, pH, initial adsorbate concentration, contact time, etc. could affect the adsorption process. The correlation between these factors and the response of interest (removal efficiency of adsorbate) can be evaluated using response surface methodology (RSM).^[19] Recently, RSM has been widely used for system performance optimization.^[20] The performance of the adsorption process can also be predicted using the artificial neural network (ANN) technique. ANN is mainly consisting of input layers (environmental factors), hidden layers, and an output layer (removal efficiency). ANN contains highly interconnected neurons that are capable of solving complex problems by linking the independent variables (inputs) with each other and with the dependent variable (output).^[21]

The main purpose of this research is to explore the effect of bimetallic Fe/Cu nanoparticles on the removal efficiency of heptachlor pesticide from aqueous solution. The effects of different environmental factors (*i.e.*, bimetallic Fe/Cu dosage, initial heptachlor concentration, pH, contact time, and stirring rate) on the adsorption process were identified using the batch technique. Isotherm and kinetic models were employed to simulate the adsorption data. RSM and ANN were also applied to find the correlation between the experimental factors and heptachlor removal efficiency.

Materials and methods

Preparation of heptachlor solution

A standard 40098 SUPELCO heptachlor solution (1,4,5,6,7,8,8-Heptachloro-3a,4,7,7a-tetrahydro-4,7-methanoindene) with concentration $1000 \mu\text{g mL}^{-1}$ in methanol, which has been purchased from SUPELCO, PA, USA, was used to prepare the stock and working heptachlor solution.

Preparation of nanoscale zero-valent iron (nZVI)

The ZVI nanoparticles were prepared by the sodium borohydride (NaBH_4) reduction method as described in a study by Cumbal and SenGupta^[22] and Zin *et al.*^[23]. About 2.4345 g iron chloride hexahydrate ($\text{FeCl}_3 \cdot 6\text{H}_2\text{O}$) that is equivalent to 0.018 M ferric chloride solution was dissolved in a 6/1 (v/v) ethanol/water mixture (417 mL

ethanol 95% + 83.0 mL deionized water) and efficiently stirred. The NaBH_4 solution was prepared by mixing 1.40 g NaBH_4 with 50 mL of deionized water. $\text{FeCl}_3 \cdot 6\text{H}_2\text{O}$ was purchased from Loba Chemie Pvt Ltd, India, and NaBH_4 was procured from WinLab Co., UK. The NaBH_4 solution was filled into the burette and then the burette was fixed above the $\text{FeCl}_3 \cdot 6\text{H}_2\text{O}$ solution and adjusted at flow rate of one drop per 2 s. The black precipitate appeared after dropping about 4 mL of NaBH_4 solution, this black precipitate quickly disappeared and appeared again in all the solution after adding approximately 23 mL of NaBH_4 . A filtration technique was used to separate the black iron nanoparticles from the liquid solution. The black iron nanoparticles were placed in two sheets of Whatman filter papers (41 circles, diameter 150 mm). After filtration, the iron nanoparticles were washed five times with 30 mL of absolute ethanol (99.99%, HPLC grade) to prevent the rapid oxidation of nZVI. Finally, the prepared iron nanoparticles were dried in the oven for 3 h at 70°C . For storage purposes, a thin layer of ethanol was added above the iron nanoparticles to prevent the oxidation of iron.^[24]

Preparation of bimetallic Fe/Cu nanoparticles

The bimetallic Fe/Cu nanoparticles were prepared according to a study conducted by Zin *et al.*^[23] About 1 g from freshly prepared nZVI was added into copper sulfate ($\text{CuSO}_4 \cdot 6\text{H}_2\text{O}$) solution in a flow rate of 0.1 g per 60 s with powerful stirring. The $\text{CuSO}_4 \cdot 6\text{H}_2\text{O}$ solution was prepared by mixing 0.1 g from CuSO_4 with 100 mL ethanol/distilled water (1:1) at 60°C . After that, the solution was allowed to settle for 15 min. The color of black nZVI was changed into coppery color. The solution was filtrated using two sheets of Whatman filter papers (41 circles, diameter 150 mm). After filtration, the bimetallic Fe/Cu nanoparticles were washed two times with 20 mL of absolute ethanol (99.99%, HPLC grade). The prepared Fe/Cu nanoparticles were dried in the oven for 5 h at 60°C . For storage purposes, a pure nitrogen gas was added above the Fe/Cu nanoparticles; the bottle was tightly closed and covered with the thin parafilm layer.

Batch adsorption studies

Adsorption of heptachlor onto bimetallic Fe/Cu nanoparticles was studied using a batch technique in 1000 mL Erlenmeyer flasks at fixed temperature of $25 \pm 2^\circ\text{C}$. A one-variable-at-a-time approach was used to examine the effects of bimetallic Fe/Cu dosage (0.05–0.40 g/L), pH (2–12), contact time (5–60 min), stirring rate (50–300 rpm), and initial heptachlor

concentration (0.5–3 µg/L) on the removal efficiency of heptachlor. The investigated factors and their ranges of variation were selected based on the literature survey.^[12,25] Experiments were performed in triplicate. Reciprocating Shaker (Digital GFL-3018, Germany) was used to mix the bimetallic Fe/Cu nanoparticles in aqueous solutions. After equilibration, the suspension of the adsorbent was separated from solution by filtration using Whatman No. 42 filter paper and the concentration of heptachlor remaining in solution was measured using Master DANI GC (fast gas chromatography) using micro column DN5 non-polar diameter 60 m × 0.32 µm × 0.25 mm, wool linear 2 mm, split/splitless injector and FID detector according to ASTM 2005 standard method for water and wastewater.^[26]

The removal efficiency of heptachlor by bimetallic Fe/Cu nanoparticles was estimated using Eq. (1):

$$R(\%) = \frac{C_o - C_f}{C_o} \times 100 \quad (1)$$

where $R(\%)$ is the heptachlor removal efficiency (%), C_o is the initial concentration of heptachlor (mg/L), and C_f is the final concentration of heptachlor (mg/L).

The adsorption capacity of heptachlor onto bimetallic Fe/Cu nanoparticles was estimated using Eq. (2):

$$q = \frac{(C_o - C_f) \times V}{W} \quad (2)$$

where q is the quantity of heptachlor adsorbed per unit mass of bimetallic Fe/Cu nanoparticles (mg/g), C_o is the initial concentration (µg/L), C_f is the concentration of Heptachlor at time t (µg/L), W is the mass of bimetallic Fe/Cu nanoparticles (g), and V is the volume of aqueous solution (L).

Characterization of nZVI and Fe/Cu nanoparticles

Prepared nZVI and Fe/Cu nanoparticles were analyzed using X-ray powder diffraction (XRD). After placing the nZVI and bimetallic Fe/Cu nanoparticles in the stainless steel sample holder, the XRD patterns were recorded at radiation wavelength (Cu K-alpha = 1.5418 Å). The X-ray current and voltage values were 40 kV and 40 mA, respectively. The diffraction angle (2θ) ranged from 5° to 70° at a step size of 0.0167°.^[27] The crystallite size of the prepared nanoparticles was calculated using Scherrer equation (Eq. (3)).^[28]

$$D = \frac{K\lambda}{\beta \cos \theta} \quad (3)$$

where D is the crystallite size (nm), θ is diffraction angle, β is the full wave at half maximum (FWHM), λ is X-ray wavelength, and K is Scherrer constant (0.9).

The surface structure of bimetallic Fe/Cu nanoparticles, before and after treatment, was investigated using Field Emission Scanning Electron Microscopy (FE-SEM) (Philips, Quanta FEG 250, USA) at voltage 20 kV and magnification 16,000 ×.

Adsorption isotherm

Isotherm study is used to describe the transmission of heptachlor from the aqueous solution phase to the solid phase of bimetallic Fe/Cu at equilibrium condition.^[29,30] The equilibrium isotherm of heptachlor was determined using nonlinear isotherm models. The nonlinear models include Langmuir, Freundlich, Redlich–Peterson, Hill, Sips, Khan, Toth, Koble–Corrigan, Jovanovich, and Hossein. The description and the nonlinear mathematical equation of each isotherm model is presented in Supplementary Table S1.

Kinetic studies

Kinetic models were used to describe the kinetics adsorption of heptachlor onto bimetallic Fe/Cu. These models include pseudo-first order, pseudo-second order, Elovich, Avrami, and Intraparticle models.^[31] The description, as well as the nonlinear equations of these models, is presented in Supplementary Table S2.

Validation of adsorption isotherms and kinetics

Five error function equations that are listed in Supplementary Table S3 were used to evaluate the better fit of nonlinear isotherm and kinetic models and to choose the most suitable model that can describe the treatment process.

Quality control

All experiments were conducted triplicate during this research and the average values are reported along with the standard deviations.^[32] Blank samples which only contain heptachlor compound without bimetallic were run along the tests. The analytical glassware[A] type and the deviation were added in uncertainty. Instruments and tools were calibrated a month before the measurements. Microsoft excels 2007; Origin 5.0, SPSS, and MATLAB software were used for all statistical analyses.

Statistical analysis

RSM is an effective tool for estimating the effects of different parameters in the removal efficiency of a specific contaminant. A linear regression equation was used to fit the laboratory batch experiment results (Eq. (4)).^[33]

$$Y = \beta_0 + \beta_1 x_1 + \beta_2 x_2 + \beta_3 x_3 + \beta_4 x_4 + \beta_5 x_5 \quad (4)$$

This relation describes the effect of studied parameters, which include pH, adsorbent dose, contact time, initial concentration, and stirring rate in the removal efficiency of heptachlor compound.^[34,35] Where β_0 is the equation constant; $\beta_{1,2,3,4,5}$ is corrected operating parameter values; $x_{1,2,3,4,5}$ is operating parameter values, and Y describes the removal efficiency.

Artificial neural network

ANN structure

The removal efficiency of heptachlor is estimated through a series of layers: input, hidden, and output. The input layer includes the data of the five studied parameters: pH, initial heptachlor concentration, contact time, stirring rate, and adsorbent dose. The hidden layer includes ten neurons, and thus a structure of 5–10–1 was used for predicting heptachlor removal efficiency. Input and target data were divided: 60% for training the network, 20% for model validation, and 20% for testing the created network.

ANN properties

The mean squared error (MSE) in feedforward back-propagation algorithm was calculated in order to compare output data with the target data (Eq. (5)).^[36] The MSE was propagated back from the output to the input layer for adjusting the values of weights and biases until reaching the maximum number of iterations:

$$MSE = \frac{\sum_{i=1}^N (t_i - a_i)^2}{N} \quad (5)$$

where N is the number of measured data, and t_i and a_i are the target data and the predicted outputs, respectively.

The algorithm method used for network training is Levenberg–Marquardt algorithm (trainlm). The transfer functions chosen for hidden layer and output layer are “tansig” which is used for pattern recognition (Eq. (6))^[36] and “purlin” which is used for function fitting (Eq. (7)),^[36] respectively:

$$f(x) = \frac{e^x - e^{-x}}{e^x + e^{-x}}, -1 \leq f(x) \leq 1 \quad (6)$$

$$f(x) = x, -\infty < f(x) < +\infty \quad (7)$$

Results and discussion

Characterization of nZVI and Fe/Cu nanoparticles

Figure 1(a) shows the XRD pattern for nZVI and Fe/Cu nanoparticles with an angle (2θ) from 5 to 70. The XRD pattern for prepared nZVI (Fig. 1(a)) shows two peaks at $2\theta = 44.58^\circ$ and 64.99° for planes Fe (110) and Fe (200), respectively. A sharp peak at $2\theta = 44.58^\circ$ indicated a dominance of zero-valent iron (Fe^0) in the prepared nZVI samples.^[20] According to XRD peak analyses (Fig. 1(a)) of prepared Fe/Cu nanoparticles, the peaks were relatively broadened and they have different intensities. These peaks are composing phases of copper and iron, and were consisting mainly of copper oxide (Cu_2O) with a small fraction of iron oxide (Fe_2O_3). The peaks with 2θ values of 29.6° , 36.5° , and 61.5° correspond to the planes of 110, 111, and 220 of crystalline Cu_2O , respectively, which agrees with the work of Qian *et al.*^[37] These results prove that the iron was encapsulated in a shell of Cu_2O . The other peaks are negligible compared with the peaks of Cu_2O , indicating that there is a little impurity.

The crystallite size of nZVI and Fe/Cu nanoparticles can be calculated using Debye-Scherrer formula through analyzing the positions and the broadness of the peaks. The FWHM for $2\theta = 44.58^\circ$ and 64.99° was 0.0067 and 0.002898 radian, respectively, and thus the calculated particle size for nZVI ranged from 23 to 59 nm, which agrees with the results obtained by the SEM analysis for nZVI nanoparticles (Fig. 1(b)). The SEM image of the synthesized nZVI showed the presence of large nanoclusters that are formed due to magnetic forces among the iron nanoparticles. The prepared iron nanoparticles have also an irregular surface structure with particle size ranging from 25 to 60 nm. There are voids spaces formed by particles stacking were observed in the SEM image which guarantees better diffusion and mass transfer of heptachlor to the inner iron nanoparticles. The crystallite size of Fe/Cu nanoparticles was estimated also using Debye-Scherrer formula from the width of the Cu (111) and Cu (200) peaks. The particle size of Fe/Cu nanoparticles ranged from 20 to 30 nm, which means that the crystallite size of Fe/Cu nanoparticles will not exceed 80 nm, which agrees with the results obtained by the SEM analysis for Fe/Cu nanoparticles (Fig. 1(c)). The SEM

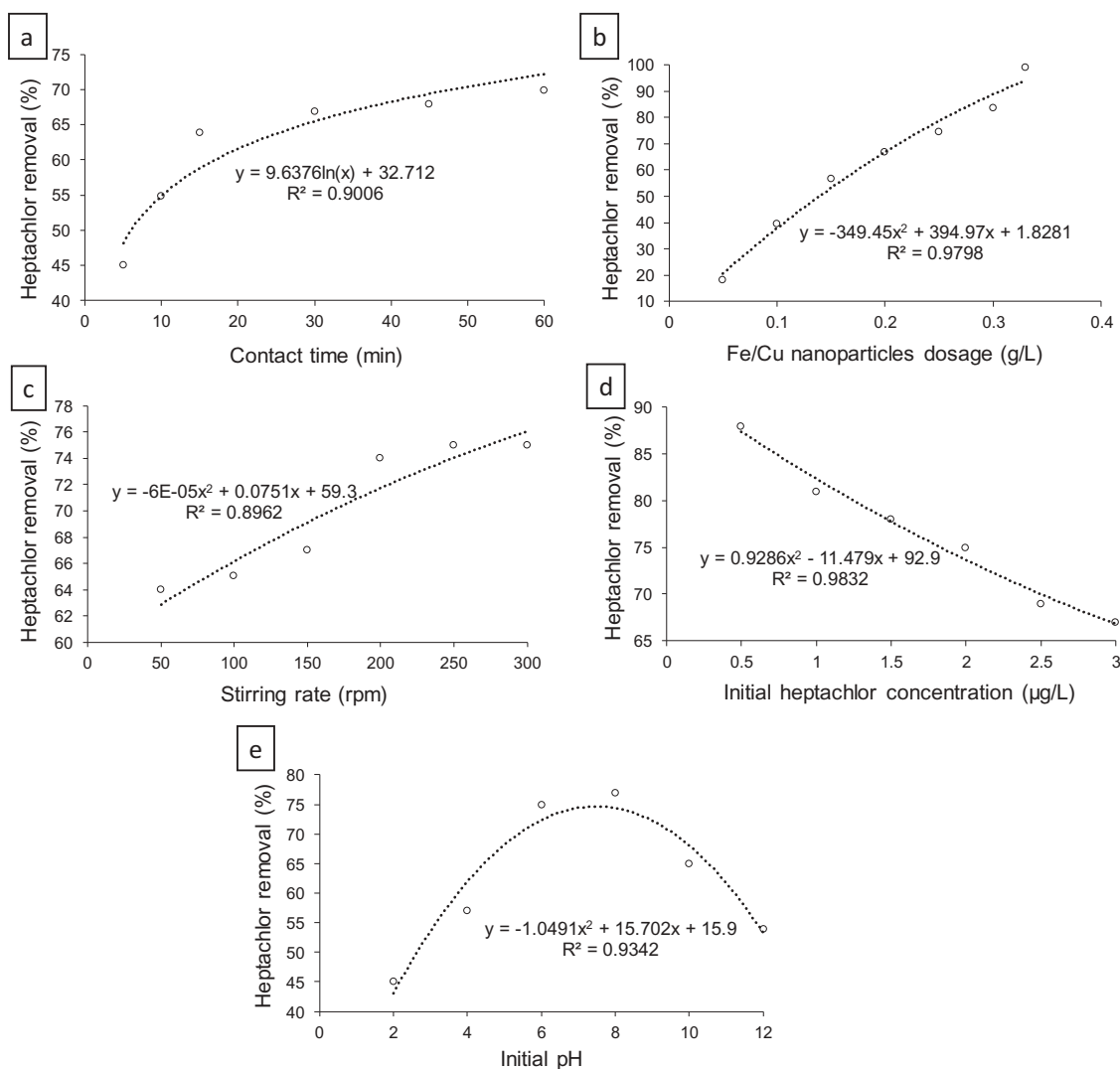


Figure 2. Effect of operating parameter on heptachlor removal using bimetallic Fe/Cu nanoparticles: (a) contact time, (b) adsorbent dose, (c) stirring rate, (d) initial heptachlor concentration, and (e) pH.

contact time was fixed at 30 min. The pH was adjusted to 7 ± 0.2 and stirring rate was fixed at 250 rpm.

The removal efficiency of heptachlor increased from 18% to 75% when Fe/Cu nanoparticles dosage was increased from 0.05 to 0.25 g/L, respectively, as shown in Fig. 2(b). This may be attributed to the increase in the number of vacant sites and the adsorbent surface with increasing the adsorbent dosage, which adsorbs great amounts of heptachlor compound.^[40] The increase of the adsorbent dosage will also increase the free electrons resulted from the separation between iron and copper nanoparticles in the solution, and thus enhance the degradation of heptachlor compounds, which in turn enhance the adsorption process.^[41] A minor improvement in the removal efficiency of heptachlor from 97% to 99% was achieved after increasing the Fe/Cu nanoparticles dosage from 0.35 to 0.4 g/L, which may be due to the agglomeration of

iron nanoparticles. Similarly, Seyhi *et al.*^[42] found that heptachlor removal by activated carbon (AC) produced from an agro-waste material was improved from 92% to 97% when the AC dosage was increased from 1 to 2 g/L, respectively.

Effect of stirring rate

The effect of stirring rate on heptachlor removal was studied at stirring rate ranges from 50 to 300 rpm. An adsorbent dosage of 0.2 g was added to 1000 mL of heptachlor. The pH was adjusted to 7 ± 0.2 and contact time was fixed at 30 min.

The removal efficiency of heptachlor increased from 64% to 75% when stirring rate was increased from 50 to 250 rpm, respectively, as shown in Fig. 4(c). This result indicated that a stirring rate of 250 rpm allows better

diffusion and transfer of heptachlor compounds into the porous of the adsorbent. In addition, no significant improvement in heptachlor removal efficiency was achieved with further increasing stirring rate to 300 rpm, where the attachment mechanism became unstable due to the disturbance that occur to the electrostatic forces within the system during high stirring rate.^[43]

Effect of the initial concentration

The effect of initial concentration on heptachlor removal was studied at initial concentration ranges from 0.5 to 3 µg/L. An initial heptachlor concentration of 2 µg/L was used along with 0.2 g of Fe/Cu nanoparticles added to 1000 mL of heptachlor and stirring rate was fixed at 250 rpm. The pH was adjusted to 7 ± 0.2 and contact time was fixed at 30 min.

The removal efficiency of heptachlor was 88% at initial concentration of 0.5 µg/L, which decreased to 67% at initial concentration of 3 µg/L, as shown in Fig. 2(d). At low concentration, the ratio of nanoparticles active sites to adsorbate compounds was high, causing more heptachlor compounds to come into contact and attach to the adsorbent surface.^[36] However, at high concentration, the removal efficiency decreased because the number of active sites was not enough to accommodate all heptachlor compounds found in the solution. In addition, the competition that exists between the heptachlor compounds to fill the pores.^[44] In another study, Ozcan *et al.*^[45] found that at initial concentration of 5 µg/L, the removal efficiency of heptachlor by montmorillonite was 96% under equilibrium time of 2 hours. The equilibrium time in most of the previous research was considerably higher than the equilibrium time reported in this study, and this is mainly attributed to the treatment mechanism. In the previous research, they focused only on adsorption, however in this study; both degradation and adsorption processes have been investigated, which in turn helps to reach equilibrium in the shortest time.

Effect of pH

The effect of pH on heptachlor removal was studied at pH ranges from 2 to 12.^[12] An initial heptachlor concentration of 2 µg/L was used along with 0.2 g of Fe/Cu nanoparticles added to 1000 mL of heptachlor. The contact time was fixed at 30 min and stirring rate was fixed at 250 rpm.

The lowest removal efficiency of heptachlor of 45% was reported at pH of 2, as shown in Fig. 2(e). At a high acidic medium, some iron nanoparticles dissolve in the

solution leading to a decrease in sorbent capacity.^[36] Another reason for the decrease in heptachlor removal efficiency is the combination of the excess H^+ found in the solution and the free electrons generated by iron nanoparticles forming water.^[36] An increase in pH from 2 to 7 resulted in an improvement of heptachlor removal efficiency from 45% to 75%, respectively. This is mainly due to the increase in the number of OH^- ions, which enhance the degradation process of heptachlor compounds. Similarly, Mansourieh *et al.*^[38] reported that the optimum pH for organophosphorus profenofos pesticide removal using bimetallic Fe/Cu was 7.

The highest removal efficiency of 77% was reported at pH 8 which is higher than the point of zero charge ($pH_{ZPC} \approx 7.7$ for nZVI.^[36] At solution pH higher than pH_{ZPC} , the nZVI surface becomes (-) in charge, which enhances the degradation and attraction mechanisms.^[34] An increase in pH level from 8 to 12 caused a decrease in heptachlor removal efficiency from 77% to 54%, respectively. This is mainly attributed to the excess OH^- ions in the solution which compete with heptachlor anions to attach to the vacant sites on the nZVI surface, as well as electrostatic repulsion that occurs between OH^- ions produced by nZVI and OH^- ions in the solution.^[44] Another reason for such a decrease in heptachlor removal efficiency in alkaline medium is the hydrolysis/corrosion of nZVI producing ferric iron and ferrous iron which precipitates in the solution as iron hydroxides/oxides.^[46]

Adsorption study

Supplementary Figure S1a describes the nonlinear relations between different adsorption isotherm models. The resulted data from adsorption study using different nonlinear models indicating that Koble–Corrigan is the most suitable model that describes the adsorption process with the lowest sum of error of 1.671, as shown in Table 1. The low sum of error suggested the consistency of Koble–Corrigan isotherm to the experimental data, as well as, the dominance of both mono and multilayer adsorption, since Koble–Corrigan model combines Langmuir and Freundlich adsorption isotherm models. This indicated that the model constants for Langmuir isotherm (*i.e.*, $K_L = 1.938 \text{ L}/\mu\text{g}$ and $q_m = 10.08 \mu\text{g}/\text{g}$) were suitable for describing the homogeny adsorption process. Furthermore, the value of $1/n$: 0.52 from the Freundlich isotherm was smaller than 1 indicating the favorable adsorption of heptachlor compounds onto nZVI at the investigated conditions. In addition, the high value of K_f : $10.08 (\mu\text{g}/\text{g}) \cdot (\text{L}/\mu\text{g})^{1/n}$ from the Freundlich isotherm indicated that the iron nanoparticles provided a great ability to adsorb heptachlor compounds.

Table 1. It shows the results of nonlinear adsorption mode.

Model	Redlich Peterson		Hill		Sips		Khan		Toth	
Constants	Kr	31.31	QH	0.053	Qs	22.27	Qk	4.498	Kt	3.758
	Br	2.21	nH	-0.004	Ks	0.734	Bk	9.768	at	0.451
	G	2339	KD	-0.99	Bs	0.732	Ak	0.627	t	3.758
Errors										
Chi error	0.259		0.741		0.055		0.084		0.259	
ERRSQ	0.639		2.025		0.286		0.349		0.638	
HYBRD	0.199		0.583		0.053		0.079		0.199	
MPSD	0.079		0.216		0.014		0.024		0.079	
ARE	0.424		0.726		0.241		0.300		0.424	
EABS	1.694		2.798		1.220		1.379		1.693	
Error sum	3.293		7.090		1.870		2.215		3.292	
Model	Koble –Corrigan		Javanovic		Hossein		Freundlich		Langmuir	
Constants	A	15.49	Qm	10.458	r	21.008	K _f	10.08	q _m	14.123
	B	0.557	Kj	2.553	p	-17.11	n	1.938	K _L	2.217
	D	0.674			z	-0.019				
Errors										
Chi error	0.044		0.455		1.278		0.059		0.259	
ERRSQ	0.273		0.963		2.764		0.373		0.638	
HYBRD	0.044		0.312		0.781		0.058		0.199	
MPSD	0.009		0.127		0.281		0.011		0.079	
ARE	0.200		0.486		0.932		0.213		0.424	
EABS	1.102		1.848		3.894		1.177		1.693	
Error sum	1.671		4.191		9.930		1.891		3.292	

Kinetics studies

Supplementary Figure S1b describes the nonlinear relations between different kinetic models. The resulted data from the kinetic study using different nonlinear models indicating that Avrami is the most suitable model that describes the adsorption process with the lowest sum of error of 0.829, as shown in Table 2. The low sum of error suggested the consistency of Avrami model to the experimental data. According to Avrami model, chemical reaction rate is an important factor that controls the kinetic process where n , a parameter depending on the nucleation mechanism and the number of growth dimension, lies between 0.5 and 1 which means that the type of nucleation and geometry of growing obey diffusion law, which lead to instantaneous nucleation and one-dimensional growth.^[47]

Statistical analysis

From the previous results, it was concluded that the effect of stirring rate in the heptachlor pesticide removal efficiency is minor. The effect of stirring rate, Fe/Cu nanoparticles dose, initial heptachlor concentration, pH, and contact time in the heptachlor removal efficiency was studied. Table 3 illustrates a positive linear effect of the independent variables “adsorbent dose,” “pH,” and “contact time,” while a negative linear effect was observed for “initial heptachlor concentration.” A significant effect ($p < 0.05$) was observed for the linear terms of “adsorbent dose,” “pH,” “initial heptachlor concentration,” and “contact time,” while insignificant effect ($p > 0.05$) was observed for the linear term of “stirring rate.”

A moderate correlation is suggested between simulated results and measured data, where the coefficient of determination (r^2) and adjusted r^2 were 0.774 and 0.720, respectively. High r^2 -value indicated that the proposed model is reliable. Eq. (8) showed the regression equation, which includes all the factors (significant and insignificant). For simplicity, the insignificant factor “stirring rate” was excluded from Eq. (8), and a new regression equation was obtained (Eq. (9)):

$$Y = -3.328 + 2.999x_1 + 261.033x_2 - 10.213x_3 + 0.402x_4 + 0.014x_5 \quad (8)$$

$$Y = 0.808 + 2.935x_1 + 260.090x_2 - 10.307x_3 + 0.4x_4 \quad (9)$$

where Y is the predicted response of heptachlor removal efficiency (%); x_1 is initial pH values (2–12); x_2 is adsorbent dose (0.05–0.4 g/L); x_3 is initial heptachlor concentration (0.5–3 $\mu\text{g/L}$); x_4 is contact time (5–60 min), and x_5 is stirring rate (50–300 rpm).

Artificial neural network

Adjusted weights and biases

The connection between each component of the input vector ($P_{5 \times 1}$) and each hidden layer neuron has generated a weight matrix ($W_{10 \times 5}$), as shown in Fig. 3a. The weighted input ($\Sigma W_{10 \times 5} \cdot P_{5 \times 1}$) was added to 10-length bias ($b_{10 \times 1}$) to produce a net input ($u_{10 \times 1} = \Sigma W_{10 \times 5} \cdot P_{5 \times 1} + b_{10 \times 1}$), which is then transferred to output layer

Table 2. The results of different kinetic models.

Model	P.F.O	P.S.O	Elovich	Avrami	Intraparticle
Constants	$Q_e = 6.787$	$Q_e = 0.498$	$\alpha = 27.863$	$Q_e = 6.905$	$K_{id} = 0.402$
Errors	$K_1 = 0.194$	$K_2 = 0.645$	$\beta = 1.033$	$K_{av} = 0.309$ $N_{av} = 0.745$	$C_i = 4.184$
Chi error	0.035	0.019	0.088	0.013	0.182
ERRSQ	0.191	0.120	0.500	0.078	1.025
HYBRD	0.034	0.019	0.086	0.012	0.185
MPSD	0.006	0.003	0.015	0.010	0.035
ARE	0.152	0.102	0.243	0.002	0.358
EABS	0.846	0.617	1.428	0.624	2.045
Error sum	1.266	0.882	2.360	0.829	3.831

Table 3. *t* statistics and *p*-values for coefficients of a linear regression model.

ANOVA						
	Model	Sum of squares	df	Mean square	F	Sig.
1	Regression	4437.604	5	887.521	14.403	0.000
	Residual	1294.026	21	61.620		
	Total	5731.630	26			
Term	Estimate	Standard error	t-ratio	Prob> t	Effect*	
β_0	-3.328	17.148	-.194	.848	Significant	
β_1	2.999	1.114	2.691	.014	Significant	
β_2	261.033	36.441	7.163	.000	Significant	
β_3	-10.213	3.644	-2.803	.011	Significant	
β_4	0.402	.161	2.490	.021	Significant	
β_5	0.014	.031	.451	.657	Insignificant	

Abbreviations: Standard error, the error of the estimated difference between the means; *t*-ratio, the *t*-ratio for the test of whether the estimated difference between the means is zero; Prob> |*t*|, the *p*-value for the test

*The significant levels at the 95% level ($p < 0.05$) were considered to have a greater impact on the response

^aDependent variable: %

^bPredictors: (constant), stirring rate rpm, time min, Conce ug/L, dose ug/L, PH

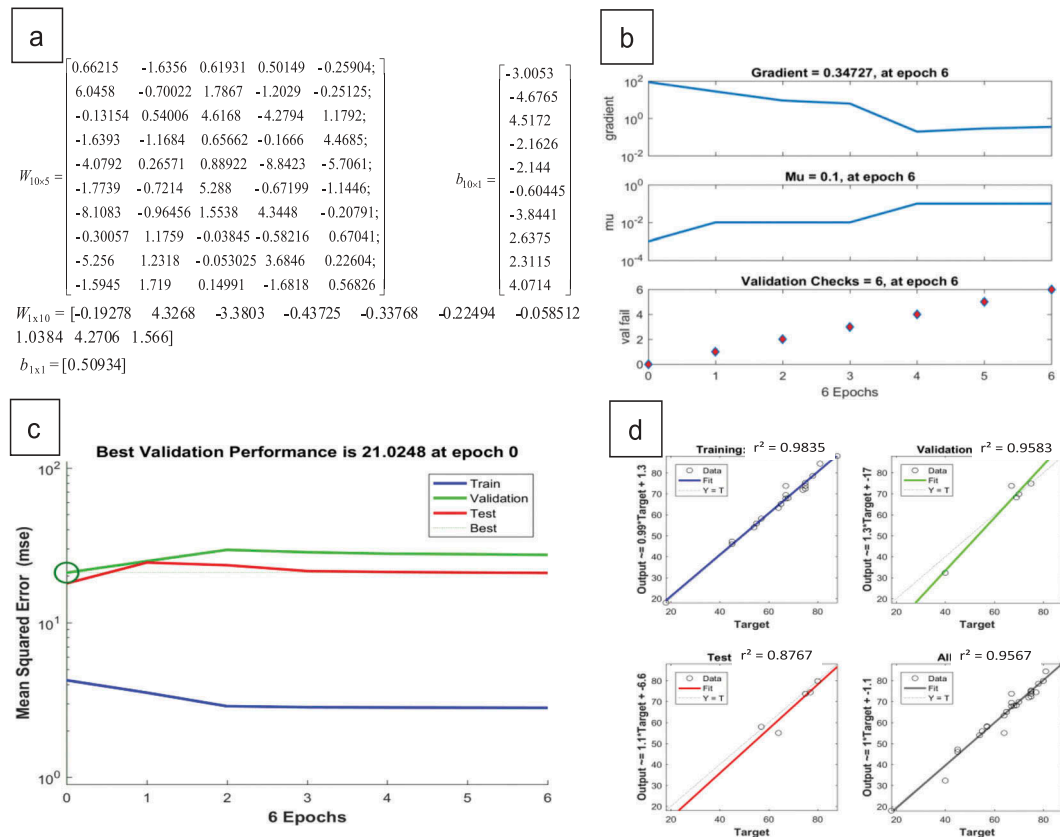


Figure 3. (a) Weight and bias matrix (b) training performance, (c) best validation performance, and (d) regression plot between target and output for the prediction of heptachlor removal efficiency.

Table 4. Testing results of RSM and ANN model with new experimental runs.

Run	Experimental parameters*					Heptachlor removal (%)			Absolute error (%)	
	x_1	x_2	x_3	x_4	x_5	Actual	ANN	RSM	ANN	RSM
1	7	0.2	2	30	100	65	65.1	62.9	0.1	2.1
2	7	0.2	2	30	150	67	69.4	63.6	2.4	3.4
3	7	0.2	2	30	200	74	71.9	64.3	2.1	9.7
4	7	0.2	2	30	250	75	73.7	65	1.3	10
5	7	0.2	2	30	300	75	75.3	65.7	0.3	9.3
6	7	0.2	2	5	250	45	46	55	1	10
7	7	0.2	2	10	250	55	55.9	57	0.9	2
8	7	0.2	2	15	250	64	63.3	59	0.7	5
9	7	0.2	2	45	250	68	68	71	0	3
10	7	0.2	2	60	250	70	69.8	77.1	0.2	7.1
11	7	0.05	2	30	250	18	18	25.9	0	7.9
12	7	0.15	2	30	250	57	58.2	52	1.2	5
13	7	0.25	2	30	250	75	74.9	78.1	0.1	3.1
14	7	0.3	2	30	250	80	79.8	91.1	0.2	11.1
15	7	0.33	2	30	250	99.3	99.4	98.8	0.1	0.4
16	7	0.2	0.5	30	250	88	88	80.3	0	7.7
17	7	0.2	1.5	30	250	78	78.5	70.1	0.5	7.9
18	7	0.2	2	30	250	75	73.7	65	1.3	10
19	7	0.2	2.5	30	250	69	68.2	59.9	0.8	9.1
20	7	0.2	3	30	250	67	67.7	54.8	0.7	12.2
21	2	0.2	2	30	250	45	47.2	50	2.2	5
22	4	0.2	2	30	250	57	58	56	1	1
23	6	0.2	2	30	250	75	72.4	62	2.6	13
24	8	0.2	2	30	250	77	74.4	68	2.6	9
25	10	0.2	2	30	250	65	65.1	74	0.1	9
26	12	0.2	2	30	250	54	54	80	0	26
	Mean absolute error								0.86	7.7

* x_1 is pH, x_2 is adsorbent dose (g/L), x_3 is initial concentration ($\mu\text{g/L}$), x_4 is contact time (min), x_5 is stirring rate (rpm)

using “tansig” function. The connection between each hidden layer neuron ($P_{10 \times 1}$) and output layer single neuron has generated weight matrix ($W_{1 \times 10}$). The weighted input ($\sum W_{1 \times 10} \cdot P_{10 \times 1}$) was added to 1-length bias ($b_{1 \times 1}$) to produce a net input ($u_{1 \times 1} = \sum W_{1 \times 10} \cdot P_{10 \times 1} + b_{1 \times 1}$), which is then transferred to output layer using “purlin” function.

Training and validation performance

The plot in Fig. 3b shows the results of the training step which include the gradient magnitude (0.34727) and the number of validation checks (6). Although the gradient magnitude has exceeded the least error level of $1e-5$, the training step was stopped because the number of validation checks has reached the maximum allowable limit at epoch 6.

Figure 3c depicts the relationship between the mean square error (MSE) performance and the iteration number. A normal trend was observed for the training step, where the MSE decreased gradually until reaching the lowest value at epoch 6. In the validation step, a gradual increase in the MSE was observed after epoch 0, which indicates over fitting of the data. A similar behavior was observed for both validation and the test curves. Finally, the best validation performance was recorded as 21.0248 at epoch 0.

Regression plot

Figure 3d depicts the relationship between network outputs and network targets. The dashed line indicates the perfect result, while the solid line indicates the best-fitting line. A very strong correlation was observed between the target and the output data in each step: training, validation and test with r^2 -values of 0.9835, 0.9583, and 0.8767, respectively. The overall r^2 -value of the three steps combined was 0.9567, indicating the reliability of the proposed model. This means that 95.67% of the variations in heptachlor removal efficiency were explained by the studied parameters (pH, adsorbent dose, initial heptachlor concentration, contact time, and stirring rate). In summary, the proposed ANN can accurately estimate heptachlor removal efficiency within the studied range.

Models verification and optimization

In order to confirm the validity of RSM and ANN models, a comparison was conducted between the outputs of these two models and the experimental results by calculating the mean absolute error (MAE) for 26 solutions (Table 4). The ANN model was found to be more reliable than RSM in predicting the removal efficiency of heptachlor, where the MAE of heptachlor removal efficiencies for 26 experimental runs when using ANN was 0.86%, while the MAE when using RSM was 7.7%.

Conclusions

Results from the batch studies conducted during this research suggest that Fe/Cu nanoparticle is a strong material that can degrade heptachlor compounds and then absorb the smaller compounds from aqueous solutions. The adsorption data fitted well by Koble–Corrigan isotherm model ($A = 15.49 \text{ L}^n \mu\text{g}^{1-n}/\text{g}$; $B = 0.557 \text{ (L}/\mu\text{g})^n$; $D = 0.674$; the sum of error = 1.671), indicating the dominance of both mono and multilayer adsorption. The adsorption data fitted also well by Avrami kinetic model, indicating instantaneous nucleation and one-dimensional growth. The highest removal efficiency for heptachlor compounds from aqueous solution was recorded as 99.3% at the following conditions: bimetallic Fe/Cu dosage of 0.33 g/L, contact time of 30 min, pH of 7.0, initial heptachlor concentration of 2 $\mu\text{g/L}$, and stirring rate of 250 rpm. Modeling results showed that ANN with r^2 -value of 0.9567 was more reliable than RSM with r^2 -value of 0.7740 in the prediction of heptachlor removal efficiency under the tested experimental conditions. At the same environmental conditions, the highest removal efficiency of 99.4% and 98.8% was recorded for ANN and RSM, respectively. This paper indicated that Fe/Cu nanoparticles are efficient in the removal of heptachlor compounds and that the designed ANN can be used in future studies to optimize the removal rate of heptachlor by Fe/Cu nanoparticles under different environmental conditions.

Disclosure statement

The authors declare that they have no conflict of interest.

Funding

This work was supported by the Egyptian Housing Building Research Center (HBRC), Zewail City of Science and Technology, and Badr University in Cairo (BUC).

ORCID

Ahmed S. Mahmoud  <http://orcid.org/0000-0003-3092-8056>

Mohamed K. Mostafa  <http://orcid.org/0000-0001-9960-3474>

References

- [1] Looser, R.; Froescheis, O.; Cailliet, G.M.; Jarman, W. M.; Ballschmiter, K. (2000) The deep-sea as a final global sink of semivolatile persistent organic pollutants? Part II: organochlorine pesticides in surface and deep-sea dwelling fish of the North and South Atlantic and the Monterey Bay Canyon (California). *Chemosphere*, 40 (6): 661–670.
- [2] Cortada, C.; Vidal, L.; Tejada, S.; Romo, A.; Canals, A. (2009) Determination of organochlorine pesticides in complex matrices by single-drop microextraction coupled to gas chromatography–mass spectrometry. *Analytica Chimica Acta*, 638 (1): 29–35. doi:10.1016/j.aca.2009.02.003
- [3] Wania, F.; Mackay, D. (1996) Tracking the distribution of persistent organic pollutants. *Environmental Science & Technology*, 30 (9): 390–396. doi:10.1021/es962399q
- [4] Arcand-Hoy, L.D.; Benson, W.H. (1998) Fish reproduction: an ecologically relevant indicator of endocrine disruption. *Environmental Toxicology and Chemistry*, 17 (1): 49–57. doi:10.1002/etc.v17:1
- [5] McLaughlin, J.; Marliac, J.P.; Verrette, M.J.; Mutchler, M.K.; Fitzhugh, O.G. (1963) The injection of chemicals into the yolk sac of fertile eggs prior to incubation as a toxicity test. *Toxicology and Applied Pharmacology*, 5 (6): 760–771. doi:10.1016/0041-008X(63)90068-1
- [6] Rodenburg, L.A.; Du, S.; Fennell, D.E.; Cavallo, G.J. (2010) Evidence for widespread dechlorination of polychlorinated biphenyls in groundwater, landfills, and wastewater collection systems. *Environmental Science & Technology*, 44 (19): 7534–7540. doi:10.1021/es1019564
- [7] Younes, M.; Galal-Gorchev, H. (2000) Pesticides in drinking water—a case study. *Food and Chemical Toxicology*, 38: S87–S90. doi:10.1016/S0278-6915(99)00132-5
- [8] Moraes, R.; Elfvendahl, S.; Kylin, H.; Molander, S. (2003) Pesticide residues in rivers of a Brazilian rain forest reserve: assessing potential concern for effects on aquatic life and human health. *AMBIO: A Journal of the Human Environment*, 32 (4): 258–263. doi:10.1579/0044-7447-32.4.258
- [9] Cassidy, R.A.; Natarajan, S.; Vaughan, G.M. (2005) The link between the insecticide heptachlor epoxide, estradiol, and breast cancer. *Breast Cancer Research and Treatment*, 90 (1): 55–64. doi:10.1007/s10549-004-2755-0
- [10] Jury, W.A.; Focht, D.D.; Farmer, W.J. (1987) Evaluation of pesticide groundwater pollution potential from standard indices of soil-chemical adsorption and biodegradation. *Journal of Environmental Quality*, 16 (4): 422–428. doi:10.2134/jeq1987.00472425001600040022x
- [11] Miles, J.; Tu, C.; Harris, C. (1969) Metabolism of heptachlor and its degradation products by soil microorganisms. *Journal of Economic Entomology*, 62 (6): 1334–1338. doi:10.1093/jee/62.6.1334
- [12] Bandala, E.R.; Andres-Octaviano, J.; Pastrana, P.; Torres, L.G. (2006) Removal of aldrin, dieldrin, heptachlor, and heptachlor epoxide using activated carbon and/or *Pseudomonas fluorescens* free cell cultures. *Journal of Environmental Science and Health Part B*, 41 (5): 553–569. doi:10.1080/03601230600701700
- [13] Joo, S.H.; Cheng, F. (2006) *Nanotechnology for Environmental Remediation*; New York, USA: Springer Science & Business Media.
- [14] Zhang, L.; Fang, M. (2010) Nanomaterials in pollution trace detection and environmental improvement. *Nano Today*, 5 (2): 128–142. doi:10.1016/j.nantod.2010.03.002

- [15] Wijesekara, S.; Harischandra, I.; Kumarathilaka, S.; Vithanage, M. (2014) Fate and transport of selection nutrients and heavy metals in nanoscale zero valent iron amended sand columns, Proceedings of the Peradeniya Univ. International Research Sessions, Sri Lanka, Vol. 18.
- [16] Harter, T. (2003) *Groundwater Quality and Groundwater Pollution*; California, USA: University of California Agriculture and Natural Resources (UCANR).
- [17] Wang, Y.; Zhao, H.; Zhao, G. (2015) Iron-copper bimetallic nanoparticles embedded within ordered mesoporous carbon as effective and stable heterogeneous Fenton catalyst for the degradation of organic contaminants. *Applied Catalysis B: Environmental*, 164: 396–406. doi:10.1016/j.apcatb.2014.09.047
- [18] Cao, J.; Xu, R.; Tang, H.; Tang, S.; Cao, M. (2011) Synthesis of monodispersed CMC-stabilized Fe–Cu bimetal nanoparticles for in situ reductive dechlorination of 1, 2, 4-trichlorobenzene. *Science of the Total Environment*, 409 (11): 2336–2341. doi:10.1016/j.scitotenv.2011.02.045
- [19] Alalm, M.G.; Nasr, M.; Ookawara, S. (2016) Assessment of a novel spiral hydraulic flocculation/sedimentation system by CFD simulation, fuzzy inference system, and response surface methodology. *Separation and Purification Technology*, 169: 137–150. doi:10.1016/j.seppur.2016.06.019
- [20] Khosravi, M.; Arabi, S. (2016) Application of response surface methodology (RSM) for the removal of methylene blue dye from water by nano zero-valent iron (NZVI). *Water Science and Technology: A Journal of the International Association on Water Pollution Research*, 74 (2): 343–352. doi:10.2166/wst.2016.122
- [21] Demuth, H.; Beale, M.; Hagan, M. (2007) *Neural Network Toolbox 5: Users Guide*; Natick, MA: The MathWorks Inc.
- [22] Cumbal, L.H.; SenGupta, A.K. (2005) Preparation and characterization of magnetically active dual-zone sorbent. *Industrial & Engineering Chemistry Research*, 44 (3): 600–605. doi:10.1021/ie040126v
- [23] Zin, M.T.; Borja, J.; Hinode, H.; Kurniawan, W. (2013) Synthesis of bimetallic Fe/Cu nanoparticles with different copper loading ratios. *Dimensions*, 13 (19): 1031–1035.
- [24] Yuvakkumar, R.; Elango, V.; Rajendran, V.; Kannan, N. (2011) Preparation and characterization of zero valent iron nanoparticles. *Digest Journal of Nanomaterials and Biostructures*, 6: 1771–1776.
- [25] Baziar, M.; Azari, A.; Karimaei, M.; Gupta, V.K.; Agarwal, S.; Sharafi, K.; Maroosi, M.; Shariatifar, N.; Dobaradaran, S. (2017) MWCNT-Fe₃O₄ as a superior adsorbent for microcystins LR removal: investigation on the magnetic adsorption separation, artificial neural network modeling, and genetic algorithm optimization. *Journal of Molecular Liquids*, 241: 102–113. doi:10.1016/j.molliq.2017.06.014
- [26] Rice, E.W.; Baird, R.B.; Eaton, A.D.; Clesceri, L.S. (2012) *Standard Methods for the Examination of Water and Wastewater*; American Public Health Association (APHA): Washington, DC, USA.
- [27] Xi, Y.; Mallavarapu, M.; Naidu, R. (2010) Reduction and adsorption of Pb²⁺ in aqueous solution by nano-zero-valent iron—a SEM, TEM and XPS study. *Materials Research Bulletin*, 45 (10): 1361–1367. doi:10.1016/j.materresbull.2010.06.046
- [28] Alexander, L.; Klug, H.P. (1950) Determination of crystallite size with the X-ray spectrometer. *Journal of Applied Physics*, 21: 137–142. doi:10.1063/1.1699612
- [29] Hu, X.J.; Wang, J.S.; Liu, Y.G.; Li, X.; Zeng, G.M.; Bao, Z. L.; Zeng, X.X.; Chen, A.W.; Long, F. (2011) Adsorption of chromium (VI) by ethylenediamine-modified cross-linked magnetic chitosan resin: isotherms, kinetics and thermodynamics. *Journal of Hazardous Materials*, 185 (1): 306–314. doi:10.1016/j.jhazmat.2010.09.034
- [30] Moradi, M.; Soltanian, M.; Pirsaeheb, M.; Sharafi, K.; Soltanian, S.; Mozafari, A. (2014) The efficiency study of pumice powder to lead removal from the aquatic environment: isotherms and kinetics of the reaction. *Journal of Mazandaran University of Medical Sciences (JMUMS)*, 23 (1): 65–75.
- [31] Moradi, M.; Mansouri, A.M.; Azizi, N.; Amini, J.; Karimi, K.; Sharafi, K. (2016) Adsorptive removal of phenol from aqueous solutions by copper (cu)-modified scoria powder: process modeling and kinetic evaluation. *Desalination and Water Treatment*, 57 (25): 11820–11834. doi:10.1080/19443994.2015.1054311
- [32] Mahmoud, A.S.; Mostafa, M.K.; Nasr, M. (2018) Regression model, artificial intelligence, and cost estimation for phosphate adsorption using encapsulated nanoscale zero-valent iron. *Separation Science and Technology*, doi:10.1080/01496395.2018.1504799
- [33] Montgomery, D.C.; Peck, E.A.; Vining, G.G. (2012) *Introduction to Linear Regression Analysis*; John Wiley & Sons. Inc: Hoboken, New Jersey, USA.
- [34] Karami, A.; Karimyan, K.; Davoodi, R.; Karimaei, M.; Sharafie, K.; Rahimi, S.; Khosravi, T.; Miri, M.; Sharafi, H.; Azari, A. (2017) Application of response surface methodology for statistical analysis, modeling, and optimization of malachite green removal from aqueous solutions by manganese-modified pumice adsorbent. *Desalination and Water Treatment*, 89: 150–161. doi:10.5004/dwt.2017
- [35] Azari, A.; Mesdaghinia, A.; Ghanizadeh, G.; Masoumbeigi, H.; Pirsaeheb, M.; Ghafari, H.R.; Khosravi, T.; Sharafi, K. (2016) Which is better for optimizing the biosorption process of lead—central composite design or the Taguchi technique? *Water Science and Technology*, 74 (6): 1446–1456. doi:10.2166/wst.2016.318
- [36] Mahmoud, A.S.; Mostafa, M.K.; Abdel-Gawad, S.A. (2017) Artificial intelligence for removal of Benzene, Toluene, Ethyl benzene and Xylene from aqueous solutions using iron nanoparticles. *Water Science & Technology: Water Supply*, 18 (5): 1650–1663.
- [37] Qian, Y.; Ye, F.; Xu, J.; Le, Z.G. (2012) Synthesis of cuprous oxide (Cu₂O) nanoparticles/graphene composite with an excellent electrocatalytic activity towards glucose. *International Journal of Electrochemical Science*, 7: 10063–10073.
- [38] Mansourieh, N.; Sohrabi, M.R.; Khosravi, M. (2015) Optimization of profenofos organophosphorus

- pesticide degradation by zero-valent bimetallic nanoparticles using response surface methodology. *Arabian Journal of Chemistry*, doi:10.1016/j.arabjc.2015.04.009
- [39] Arabi, S.; Sohrabi, M. (2014) Removal of methylene blue, a basic dye, from aqueous solutions using nano-zerovalent iron. *Water Science & Technology*, 70 (1): 24–31. doi:10.2166/wst.2014.189
- [40] Cao, D.; Jin, X.; Gan, L.; Wang, T.; Chen, Z. (2016) Removal of phosphate using iron oxide nanoparticles synthesized by eucalyptus leaf extract in the presence of CTAB surfactant. *Chemosphere*, 159: 23–31. doi:10.1016/j.chemosphere.2016.05.080
- [41] Lakshmi, P.V.; Vijayaraghavan, R. (2016) A new synergistic nanocomposite for dye degradation in dark and light. *Scientific Reports*, doi:10.1038/srep38606
- [42] Seyhi, B.; Drogui, P.; Gortares-Moroyoqui, P.; Estrada-Alvarado, M.I.; Alvarez, L.H. (2014) Adsorption of an organochlorine pesticide using activated carbon produced from an agro-wastematerial. *Journal of Chemical Technology & Biotechnology*, 89: 1811–1816. doi:10.1002/jctb.2014.89.issue-12
- [43] Hamdy, A.; Mostafa, M.K.; Nasr, M. (2018) Regression analysis and artificial intelligence for removal of methylene blue from aqueous solutions using nanoscale zero-valent iron. *International Journal of Environmental Science and Technology*, doi:10.1007/s13762-018-1677-z
- [44] Ligneris, E.; Dumée, L.F.; Kong, L. (2018) Nanofiber-based materials for persistent organic pollutants in water remediation by adsorption. *Applied Sciences*, doi:10.3390/app8020166
- [45] Ozcan, S.; Tor, A.; Aydin, M.E. (2012) An investigation on the sorption behaviour of montmorillonite for selected organochlorine pesticides from water. *Environmental Technology*, 33 (11): 1239–1245. doi:10.1080/09593330.2011.618936
- [46] Sun, X.; Kurokawa, T.; Suzuki, M.; Takagi, M.; Kawase, Y. (2015) Removal of cationic dye methylene blue by zero-valent iron: effects of pH and dissolved oxygen on removal mechanisms. *Journal of Environmental Science and Health Part A*, 50 (10): 1057–1071. doi:10.1080/10934529.2015.1038181
- [47] Criado, J.M.; Ortega, A. (1987) Non-isothermal crystallization kinetics of metal glasses: simultaneous determination of both the activation energy and the exponent n of the JMA kinetic law. *Acta Metall*, 35 (7): 1715–1721.